

# Dual-Energy Computed Tomography for Diagnosis and Monitoring Attempted Medical Management of a Large Urate Urolith in a Desert Tortoise (*Gopherus agassizii*)

Jessica M. Eisenbarth<sup>1,2</sup>, David M. Gauntt<sup>3</sup>, Anne E. Rivas<sup>2</sup>

<sup>1</sup> College of Veterinary Medicine, Department of Clinical Sciences, Auburn University, Auburn, AL 36849, USA

<sup>2</sup> Birmingham Zoo, Birmingham, AL 35223, USA

<sup>3</sup> UAB Medical Center, Department of Radiology, Birmingham, AL 35294, USA

## Abstract

An estimated 29-yr-old male zoo-housed desert tortoise (*Gopherus agassizii*) presented for endoscopic liver biopsies as part of a diagnostic workup for recurrent, profound anemia and hypoalbuminemia. Suspected cystoliths were identified during endoscopy, but were not visible on conventional radiographs. Dual-energy computed tomography (DECT) imaging confirmed the presence of a large urate urolith filling the majority of the bladder. Because of the recent clinical illness, the tortoise was considered a poor surgical candidate. Medical management consisting of urinary alkalinization with potassium citrate, vibration therapy, and daily warm water soaks was elected. Following institution of medical therapies, the tortoise began passing pieces of urate stone that were 0.25–2.0 cm in diameter during daily soaks. A recheck DECT scan at 2 months indicated the urolith was approximately one third the initial size, suggesting medical therapy was effectively treating the urolith. Unfortunately, after 5 months of medical therapy, the stone had increased in size again on the follow-up DECT scan. This case report suggests that medical management may be a potential option for large urate cystoliths in desert tortoises, although more research is needed to further refine effective therapeutics for such cases. The use of DECT imaging was essential in this case because it enabled confirmation of stone presence, identification of urolith composition, and monitoring of response to therapy.

**Key Words:** Chelonian, desert tortoise, dual-energy computed tomography, *Gopherus agassizii*, potassium citrate, urolithiasis

## Introduction

Urolithiasis is a common and serious problem in chelonians, leading to significant morbidity and mortality (Keller *et al.*, 2015). A recent retrospective case series showed that in chelonians with urolithiasis, presenting clinical signs were often nonspecific (Keller *et al.*, 2015). Although some particularly large or distal uroliths may be identified via digital palpation of the prefemoral fossa or cloaca, the diagnosis of urolithiasis is usually made via imaging such as radiography, ultrasonography, computed tomography (CT), or endoscopy (Chitty and Raftery, 2013; Keller, 2019). In reptiles, uroliths are most commonly composed of uric acid, although other types have been reported (Divers and Innis, 2019). Unlike in mammals, urate uroliths in reptiles are frequently, but not always, radiopaque, allowing for radiographic diagnosis in many

cases; this is because many urate uroliths in chelonians are frequently large and dense and often have other mineral depositions in addition to urate (Holmes and Divers, 2019). Compared with conventional radiography, CT is able to detect nearly all types of urinary calculi and is considered the gold standard of urolith diagnosis in human patients (Kambadakone *et al.*, 2010). Generally, hematology, biochemistry, and urinalysis are not especially sensitive for urolithiasis in chelonians, although exceptions are seen in cases of urinary obstruction (Divers and Innis, 2019; Keller, 2019).

Dual-energy CT (DECT) has shown promising results in helping characterize stone composition without substantial increases in radiation doses compared with the more common, unenhanced helical CT (Ravi *et al.*, 2017). Conventional single-energy CT produces images that are sensitive to the X-ray attenuation of materials, but cannot

distinguish between a low-density, high atomic number material and a high-density, low atomic number material. (Ravi *et al.*, 2017). DECT works by acquiring CT data by using two different tube voltages: a high voltage (140–150 kVp) and a low voltage (80–100 kVp) (Murray *et al.*, 2019). The difference in attenuation of calculi between the low- and high-energy scans is used to determine both the atomic number and the density of the material in question. Materials with a high atomic number have a larger change in attenuation with voltage than objects with a low atomic number (Ravi *et al.*, 2017).

In human medicine, stone composition is central to determining the recommended treatment course. For example, stones comprised of uric acid are frequently medically managed with urinary alkalization therapy and surgical removal is only warranted for those who lack response to medical therapy or have life-threatening complications (Ngo and Assimos, 2007). Human urolithiasis studies indicate that *in vivo* characterization with DECT can be achieved with 73–95% accuracy, depending on radiation dose and stone types (Hidas *et al.*, 2010; Wisenbaugh *et al.*, 2014; Leng *et al.*, 2015; Basha *et al.*, 2018). For uric acid stones, in particular, DECT has been found to be highly reliable (97.6%) in discriminating uric acid from nonuric acid calculi, although calcified calculi were difficult to discern (Basha *et al.*, 2018).

Medical treatment of urate uroliths in chelonians has not been described to the author's knowledge, and little has been published on the use of DECT to assess urolith composition in chelonians, although it has been noted that urate uroliths can have a lamellar structure on both radiographs and CT (Keller *et al.*, 2015). This case report demonstrates the value of DECT as a diagnostic tool for chelonian urolithiasis and explores potential medical management options for urate uroliths in tortoises.

## Case Report

A 29-yr-old male desert tortoise (*Gopherus agassizii*) housed in a zoological institution presented in February 2018 for veterinary evaluation after keepers reported a 700-g weight loss (17% of total body weight) over the previous month. This animal was hatched at a zoo and had been housed with a female desert tortoise since entering the collection. The tortoises were kept in a 1.8 m × 3.1 m × 1.8 m (6 ft × 10 ft × 6 ft) indoor exhibit with several basking areas and a shallow bowl. Environmental conditions were in line with those recommended for desert tortoises with temperatures ranging from 25.6 to 29.4°C (78–85°F) and humidity at 50% (Klaphake *et al.*, 2018). The diet consisted of leafy greens, such as spinach and romaine lettuce, fresh-cut vegetables, grass hay, and commercial tortoise diets (Mazuri Exotic Animal Nutrition, St. Louis, MO, USA; Repashy Pet Products, Oceanside, CA, USA).

On initial physical exam, the tortoise weighed 3.46 kg and was markedly underconditioned, with a body condition score of 2/9. It had weak muscular tone in the limbs and neck. No other abnormalities were noted on the

physical exam. Radiographs revealed an empty gastrointestinal tract, but otherwise were within normal limits. Blood collected from the left brachial vein for hematologic and biochemical analysis showed a marked anemia with a packed cell volume (PCV) of 11% (reference range: 15–39%), a total solids (TS) of 36 g/L (3.6 g/dl; reference range for total protein: 30–46 g/L), and an elevated uric acid of 1,231.3 μmol/L (20.7 mg/dl; reference range: 161–428 μmol/L; Klaphake *et al.*, 2018). The tortoise was hospitalized in an off-exhibit habitat, maintaining temperature ranges and humidity within the same ranges as the on-exhibit enclosure. Bloodwork was repeated the next day and showed a worsening PCV of 6% and a decrease in TS to 24 g/L (2.4 g/dl). The tortoise was administered 20 ml of heparinized whole blood from a conspecific female via the subcarapacial venous sinus. No crossmatching was performed. The tortoise was briefly anesthetized with alfaxalone (Alfaxan, 10 mg/ml, Jurox Inc., Kansas City, MO, USA) at 10 mg/kg IM, and an esophageal feeding tube was placed. The tortoise was administered enrofloxacin (Baytril, 22.7 mg/ml, Norbrook Laboratories Limited, Newry, Ireland) at a loading dose of 10 mg/kg IM, followed by 5 mg/kg IM every 24 h for 7 days, to treat for potential infectious causes of clinical signs. It also received iron hydrogenated dextran (iron hydrogenated dextran, 100 mg/ml, VetOne, Boise, ID, USA) at 12 mg/kg IM once; reptile Ringer's (equal parts of 5% dextrose, 0.9% NaCl, and lactated Ringer's solution; Klaphake *et al.*, 2018) 5 ml/kg SC twice daily for 7 days; and 2.5 ml/kg of an herbivore critical care diet (Emeraid Intensive Care Herbivore, 1:1 powder:water, Emeraid LLC, Cornell, IL, USA) through feeding tube, every 12 h for 2 days. Two days after transfusion, repeated PCV and TS had improved at 27% and 48 g/L (4.8 g/dl), respectively. The tortoise continued to show gradual improvement with slow return of appetite and feces. Notably, no urates were seen in the enclosure for 11 days after hospitalization, despite subcutaneous fluid therapy. However, once urates were noted on the 11th day of hospitalization, urate elimination was much more frequent. On the 17th day of hospitalization, PCV and TS measurements were repeated and were 27% and 30 g/L (3.0 g/dl), respectively. The uric acid elevation had resolved at 392.6 μmol/L (6.6 mg/dl), but a mildly elevated aspartate aminotransferase (AST) 3.02 μkat/L (182 U/L) had developed. At that time, the tortoise was gaining weight, eating consistently, and acting bright and alert; thus, the feeding tube was removed. The tortoise was returned to a nondisplay habitat. Repeat blood chemistry 1 month later was unremarkable, with normal uric acid, AST, hematocrit, and total protein.

Fourteen months later, the tortoise presented again for lethargy, inappetence, and weight loss. On physical exam, the patient was lethargic and weak, with sunken eyes and tacky mucus membranes. No other abnormalities were noted. Hematology revealed a recurrent marked anemia (PCV of 13%), decreased total solids 15 g/L (1.5 g/dl), albumin < 1 g/L (<0.1 g/dl), hypoglycemia (1.89 mmol/L; 34 mg/dl), and a mildly increased uric acid 422.3 μmol/L

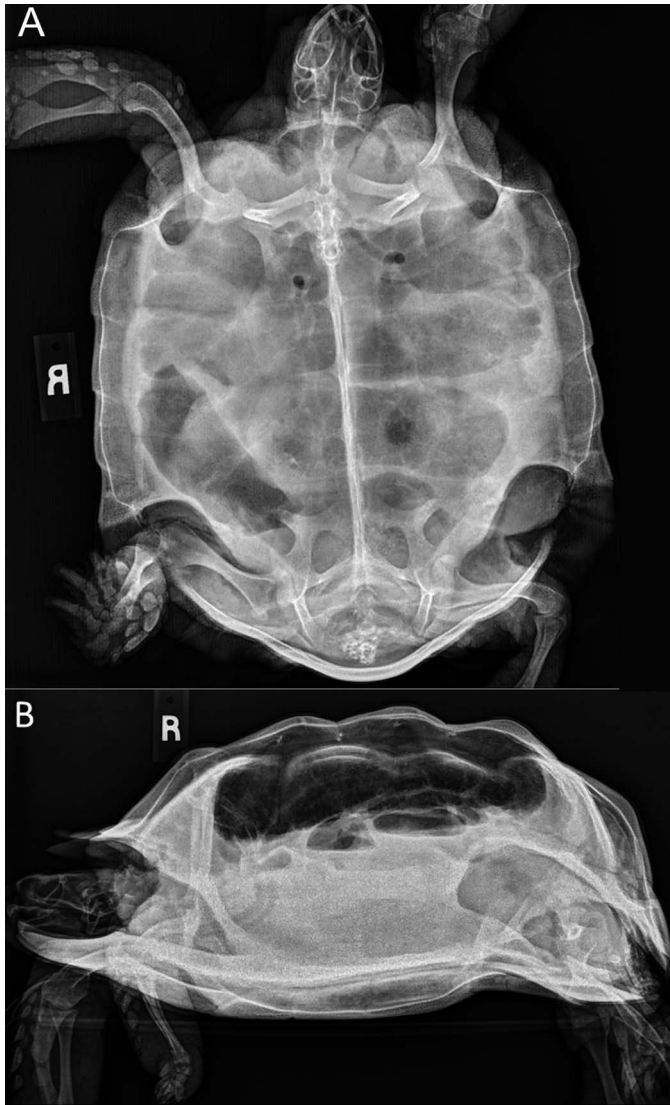


**Figure 1.** Dorsoventral (A) and lateral beam (B) radiographs of a desert tortoise (*Gopherus agassizii*) revealed an empty gastrointestinal tract, but were otherwise unremarkable. No urolith was visible on conventional digital radiographs. These radiographs were taken during the same procedure as the endoscopy images in Figure 2, which clearly show a cystolith.

(7.1 mg/dl) for a fasted animal. Radiographs taken at the time were deemed unremarkable (Fig. 1). The animal was again treated supportively and improved with intensive care. Because of the recurrent, severe anemia, low blood glucose, and hypoproteinemia, it was suspected that the animal was in acute liver failure and endoscopic liver biopsies were pursued. The tortoise was induced with alfaxalone at 9 mg/kg IV, intubated, and maintained on isoflurane (Isoflurane, 99.9%/ml, Piramal Enterprise Limited, Telangana, India). Coelioscopy was performed via the left femoral fossa with a 2.7-mm rigid 30° endoscope (Karl Storz Hopkins® II Forward-Oblique Telescope, El Segundo, CA, USA). The liver was subjectively smaller than expected, and there were multifocal areas of white depigmentation on the surface. Biopsies were taken from the grossly abnormal depigmented area and more normal

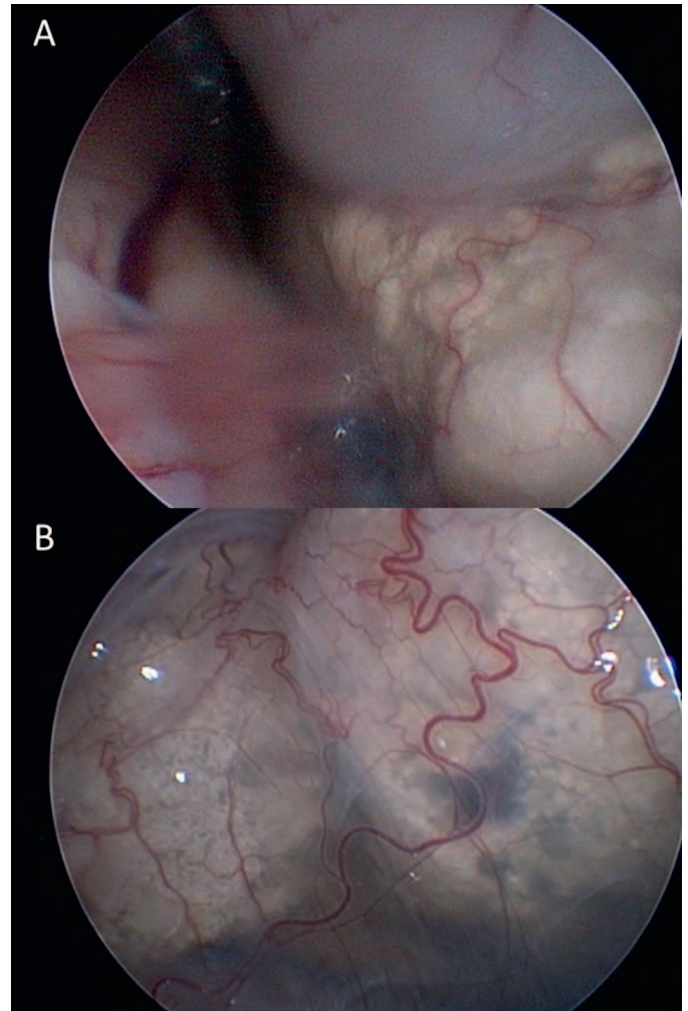


**Figure 2.** Endoscopic images acquired through a prefemoral approach of a desert tortoise (*Gopherus agassizii*). A white, gritty mass was present within the urinary bladder in the caudal coelom in both images (A) and (B). These images were taken during the same procedure as the radiographs in Figure 1, which show no evidence of a cystolith.

appearing liver adjacent to it. Within the bladder, a firm, white, lobulated mass was visualized, consistent with a urolith (Fig. 2). Meloxicam (Metacam, 5mg/ml, Boehringer Ingelheim, Duluth, GA, USA) at 0.2 mg/kg SC once, ceftiofur crystalline free acid (Excede, 100 mg/ml, Zoetis, Kalamazoo, MI, USA) at 20 mg/kg IM once, and sodium chloride 0.9% injection at 15 ml/kg SC once were administered. Recovery was uneventful. Biopsy samples were fixed in 10% buffered formalin and sent to a pathology service (University of Georgia Zoo and Exotic Animal Pathology, Athens, GA, USA). The hepatic biopsy was consistent with hepatic melanomacrophage hyperplasia and hemosiderosis. The pathologist's interpretation was that melanomacrophage hyperplasia in this case was because of emaciation or environmental or metabolic stressors and that the hemosiderosis was because of increased erythrocyte turnover. This biopsy did not indicate acute, synthetic liver failure or explain the observed clinical signs and hematology results.

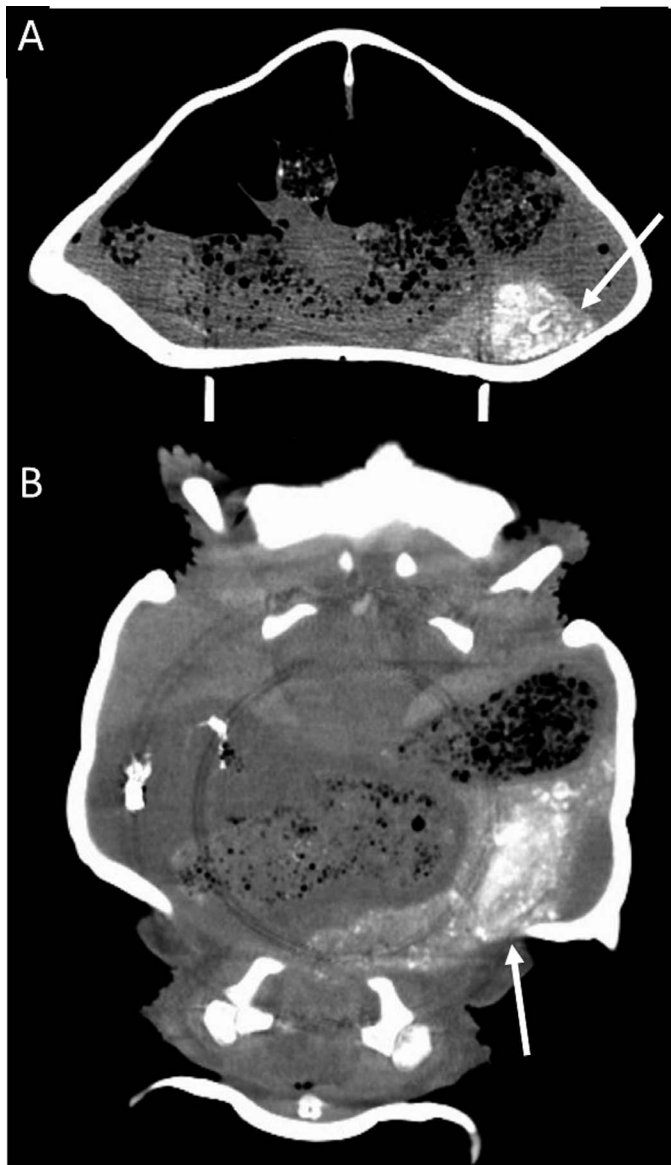


**Figure 3.** Initial dual-energy computed tomography (DECT) of a desert tortoise (*Gopherus agassizii*). Initial DECT showed a large urate urolith (arrows) in the left lobe of the bladder in both the axial (A) and coronal (B) planes. These are both 70-keV monoenergetic images.

Further diagnostics were pursued to assess the significance of the large urolith identified during the coelioscopy. Ultrasound via femoral fossa for cystocentesis revealed that the urolith occupied the majority of the visible bladder lumen. Urine collection via cystocentesis was performed, and the urine pH was 6.0 based on urine dipstick (reference range for normal urinary pH in a desert tortoise during season of presentation:  $6.9 \pm 0.05$ ; Christopher *et al.*, 1994). Nonanesthetized DECT imaging was performed to help identify stone composition. The tortoise was placed on a raised piece of PVC pipe, and the whole body was scanned. No IV contrast was used. The DECT scan (General Electric Discovery HD750 CT Scanner, Chicago, IL, USA) revealed a 11.3 cm  $\times$  4.5 cm  $\times$  3.3 cm urolith in the left bladder lobe that was consistent with urate stone

(Fig. 3). Medical management was elected before pursuing invasive surgery because this patient was deemed a poor surgical candidate because of the recent profound anemia. Medical management of the urate stone through urine alkalization therapy was attempted with potassium citrate granules (Potassium Citrate granules, 840 mg/g, NOW foods, Bloomingdale, IL, USA) at 75 mg/kg PO in soaked tortoise biscuits (Mazuri Exotic Animal Nutrition), every 24 h during the treatment period. In an attempt to aid the stone in dissolution, vibration therapy was used by attaching a personal massager (Vibrator California Exotics Novelties LLC, Ontario, CA, USA) with 7.6-cm (3-in.) bandaging tape (Vetrap, 3M, St. Paul, MN, USA) to the plastron. The device was attached and activated on the highest setting for approximately 10 min, twice daily, during the treatment period. The animal also was soaked in warm water for 20–30 min daily.

Vibration therapy was well tolerated by the patient, and there was excellent compliance with the potassium citrate. After 13 days of this treatment, the tortoise began regularly passing pieces of urate 1–2 cm in diameter during daily soaks. Over the course of a week, the pieces of urate became smaller until the tortoise was passing sand-like granules of urate during daily soaking. After 1 month of medical management, repeated cystocentesis revealed the urine pH had increased to 9, confirming alkalization of urine by the potassium citrate. Repeated DECT performed 2 months after starting treatment showed that the stone had reduced in size, measuring 4.2 cm  $\times$  1.3 cm  $\times$  0.7 cm (Fig. 4). The stone also was visualized in the right lobe of the bladder. It is thought that the reduced size of the cystoliths enabled movement from the left lobe into the right lobe of the bladder. Potassium citrate medical therapy, vibration therapy, and soaking were continued, and repeated DECT was performed 5 months after initial diagnosis. Unfortunately, the uroliths had grown to 12.4 cm  $\times$  2.7 cm  $\times$  2.9 cm overall (Fig. 5). The patient remained asymptomatic at this time, but because of overall long-term failure of medical management, a cystotomy via the standard prefemoral approach was elected. The single calculus was fragmented to facilitate removal. All of the material was removed from the bladder during the cystotomy (Fig. 6). The Minnesota Urolith Center (St. Paul, MN, USA) report indicates the stone was 100% ammonium urate. Postsurgical bloodwork did not occur as initially planned because of a global pandemic, resulting in staff scheduling changes and limiting all nonessential procedures. The cause for the anemia and other clinical signs is undetermined. However, 12 months after surgery, the tortoise remains clinically normal and maintains a healthy appetite and bright mentation.

## Discussion

Urolithiasis diagnosis methods in chelonians are variable. In a retrospective case series of 100 cases of chelonians with urolithiasis, 92 of the cases were identified during routine annual exams of asymptomatic patients

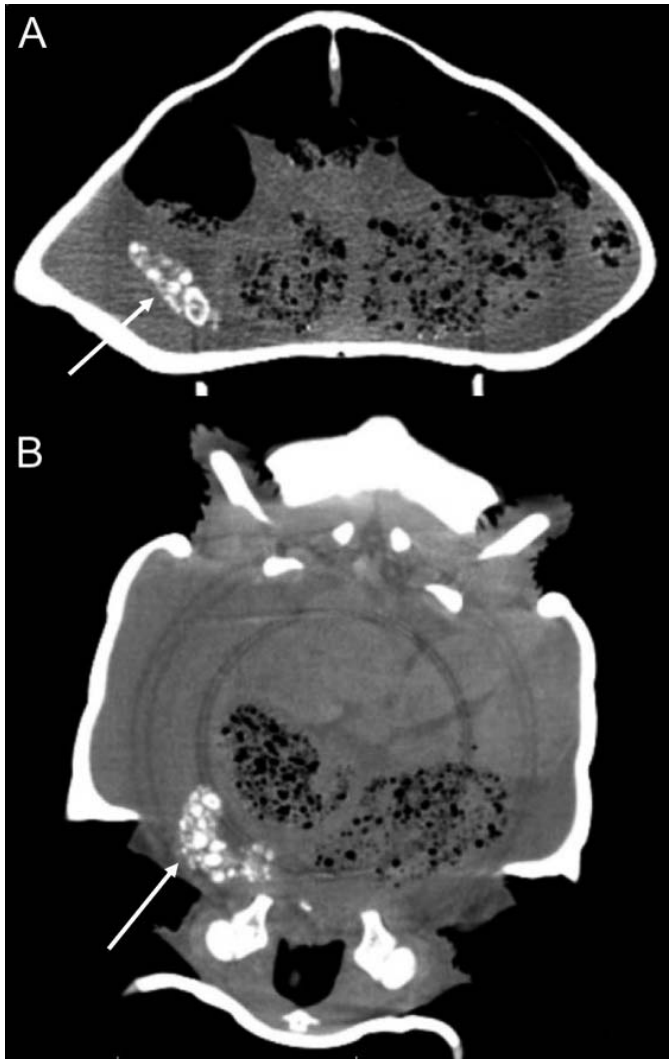


**Figure 4.** Follow-up dual-energy computed tomography (DECT) of a desert tortoise (*Gopherus agassizii*) after 2 months of urinary alkalinization treatment. DECT showed a reduction in size of the urolith (arrows) in the right lobe of the bladder in both the axial (A) and coronal (B) planes. The uroliths were reduced in size, enabling movement from the left lobe into the right lobe of the bladder.

(Mader *et al.*, 1999). This is in contrast to another retrospective study in which only 1 of the 40 animals evaluated was diagnosed at a routine annual exam (Keller *et al.*, 2015). This study also reported that stones were palpable in only 25% of the patients (Keller *et al.*, 2015). Because uroliths can be difficult to detect through palpation alone and patients can display no outward signs of disease, radiographs are recommended as part of routine, preventive health protocols in chelonians (Mader, 2005). It has been previously reported that chelonian uroliths are usually radiodense. In the retrospective study by Keller *et al.* (2015), for the 19 chelonians with radiographs available, only one had a stone that was not radiodense. In this same study, approximately one third of tortoises with uroliths were diagnosed via a CT. Only four patients had both a CT and radiographs performed,

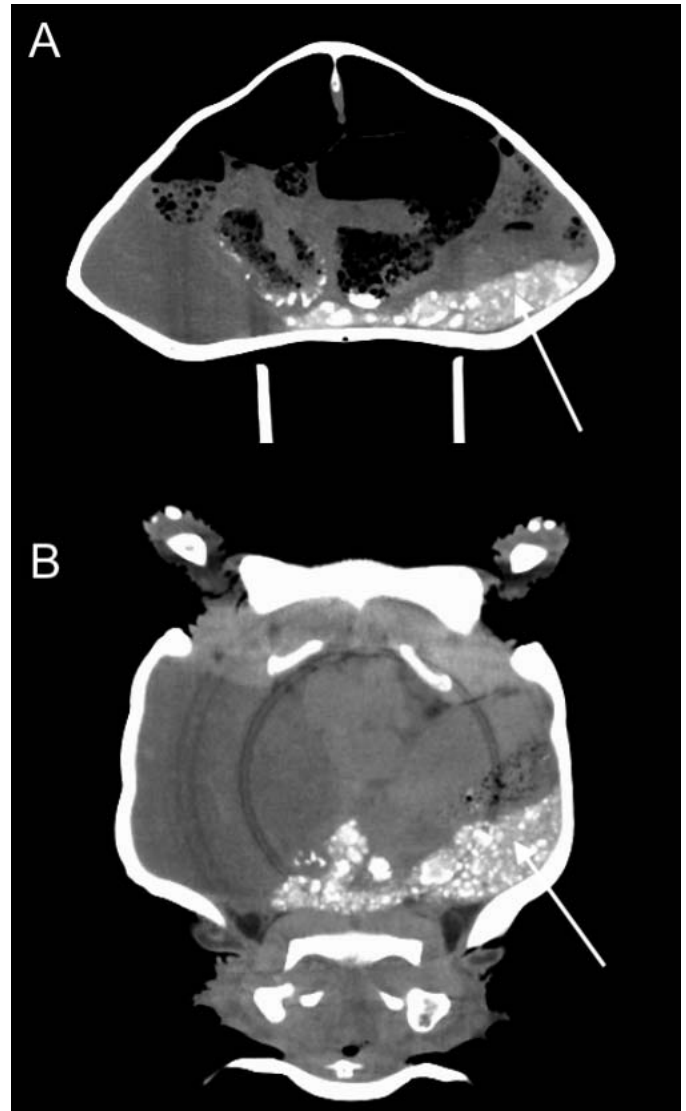


**Figure 5.** Follow-up dual-energy computed tomography (DECT) of a desert tortoise (*Gopherus agassizii*) after 5 months of urinary alkalinization treatment. DECT showed recurrence of the urolith (arrows) in the left lobe of the bladder in both the axial (A) and coronal (B) planes.

making it difficult to determine whether CT is a more sensitive diagnostic tool for urolithiasis. However, two of the four cases had additional coelomic pathology identified on CT that was not seen on radiographs (Keller *et al.*, 2015). Therefore, CT may provide information about other organ systems within the coelom that may affect the clinician's treatment plan or the patient's prognosis. As this report illustrates, it is possible for significant uroliths to not be visible on radiographs, necessitating other diagnostics modalities. DECT imaging was essential in confirming the presence, size, and location of the urolith in the desert tortoise in this case report. Furthermore, DECT noninvasively determined that the stone was a uric acid based urolith, which guided the pursuit of medical management through oral urinary alkalinization therapy.



**Figure 6.** Cystoliths removed during a cystotomy via a prefemoral approach of a desert tortoise (*Gopherus agassizii*). The single calculus was fragmented to facilitate removal. In total, 27 white, semifriable pieces ranging in size from 4 to 25 mm in diameter were removed.

DECT is not commonly used in veterinary medicine, and clinicians may not be as familiar with the imaging modality. A standard CT image of any object is an array of points (pixels), each of which has a value known as a CT number. The CT number, which has Hounsfield units (HU), is a measure of how well the material in a small volume (voxel) in the object attenuates X-rays. Materials such as bone, which attenuates X-rays well, have higher CT numbers, whereas materials such as soft tissue, which are more transparent to X-rays, have lower CT numbers. By definition, the CT number of air is  $-1,000$  HU and the CT number of water is  $0$  HU. In short, the CT number depends on three things: the density of the material, the average atomic number of the material, and the X-ray energy. Consequently, for a given X-ray energy it is possible for two materials with different densities to have the same CT number. For example, a dense bladder stone made of uric acid can have the same CT number as a less dense bladder stone containing calcium carbonate. Although the CT number depends on a combination of the material's density and atomic number, dual-energy CT is a technology that can measure density and atomic number separately. A dual-energy scanner will simultaneously produce two images: a high-energy image and a low-energy image. The low-energy image will have a much higher contrast between bone and soft tissue than the high-energy image. These images can be combined to produce images that look like conventional CT images at any arbitrary voltage, or images with pixel values that depend on density alone or atomic number alone, or material-equivalent images. For example, the General Electric Discovery CT scanner used in this case report can produce two images called water(iodine) and iodine(water) images (Fig. 7). The pixel value in the water(iodine) image is the water-equivalent density of the material in 1 voxel, whereas the

pixel value in the iodine(water) image is the iodine-equivalent density. These numbers are not the amount of water or iodine in the voxel; they will generally have nonzero values even when there is no water or iodine. Rather, they represent a mixture of water and iodine that would have the same X-ray attenuation over a wide range of X-ray energies as the material that is actually in the voxel. Therefore, based on its pixel values, the composition of a given structure in a DECT image can be determined when compared with the pixel values of known materials (i.e., urate vs. calcium carbonate).

In human medicine, DECT is being increasingly used for diagnosis and treatment planning of urolithiasis, because it allows for accurate *in vivo* characterization of uroliths, which is essential diagnostic information when determining a treatment course (Andrabi *et al.*, 2015). Currently, DECT in veterinary medicine is uncommon. In an *in vitro* model of canine uroliths, no single DECT parameter was able to differentiate the common types of uroliths (Nykamp, 2017). Taken together, however, three parameters—DECT ratio, DECT number, and low-energy CT number—could differentiate calcium oxalate, urate, and brushite uroliths, but not struvite or cystine uroliths (Nykamp, 2017). More research regarding the clinical use of DECT in veterinary medicine and validation of this method in various species are crucial to determining whether this diagnostic modality is feasible for urolith characterization in veterinary species.

Urolithiasis is commonly seen in chelonians, with urate being the predominant component in most cases (Mader, 2005; Keller *et al.*, 2015). Multiple techniques for addressing urolithiasis in chelonians have been previously reported. Surgical removal of uroliths via plastronotomy and subsequent cystotomy is perhaps the most common therapeutic, although it is not without risks (Frye, 1972; Mader *et al.*, 1999, 2005; Amat *et al.*, 2012). A retrospective of chelonian urolithiasis showed that of the 17 patients that underwent invasive management (cystotomy via plastronotomy, lithotripsy, and endoscopic-assisted digital removal through the cloaca), five developed postoperative complications, with four of these dying as a result (Keller *et al.*, 2015). Even tortoises that survived the procedure had a potential for complications. One tortoise had a lack of plastronotomy patch healing even at 4 years postoperatively (Keller *et al.*, 2015). Another tortoise presented 2 months after cystotomy via plastronotomy for not urinating for 1 month. The bladder was found to be severely distended, and urinary catheterization was unsuccessful. The animal died, and necropsy revealed severe bladder wall mucinosis and distension (Keller *et al.*, 2015). Additional complications included acute death after cystotomy via plastronotomy and humane euthanasia after multiple failed attempts of cloacolith removal via cloacoscopy (Keller *et al.*, 2015). By contrast, a retrospective of 100 desert tortoises with uroliths showed no postoperative deaths with the standard plastronotomy approach used in 90 tortoises and the inguinal fossa approach used in 10 tortoises (Mader *et al.*, 1999). Some advocate the inguinal fossa approach used in this case report over a plastronot-

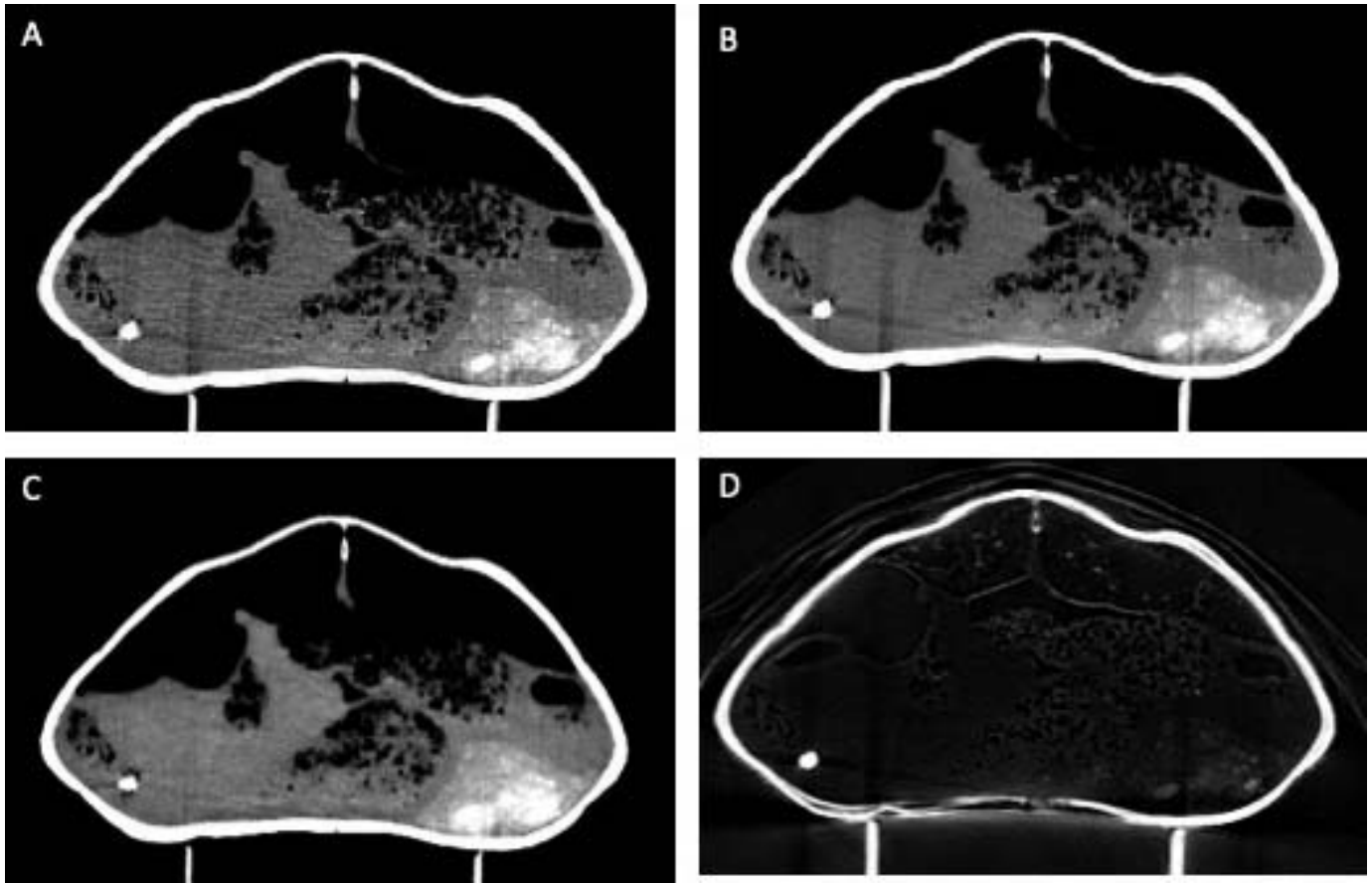


**Figure 7.** Four axial CT images of a desert tortoise (*Gopherus agassizii*). (A) Image was generated from the 140-kV acquisitions. (B) Image is the 70-keV monoenergetic image reconstructed from the 80- and 140-kV acquisitions. (C and D) Water(iodine) and iodine(water) image reconstructed from the same data. Note that the iodine(water) image allows easy differentiation between the noncalcified cystoliths on the left, and the calcification on the right.

omy because it is significantly less invasive. In an earlier study evaluating 10 chelonians that had cystoliths removed via the inguinal fossa, nine patients had no postoperative complications, although there was still one postoperative death (Mangone and Johnson, 1998). The drawback to the inguinal fossa approach for cystotomy in chelonians is more limited visualization than a plastronotomy. In the aforementioned desert tortoise retrospective study, subsequent plastronotomies performed on the 10 cases that underwent inguinal fossa cystotomies revealed that bladder rents, adhesions, and other internal pathology was missed in all 10 during the initial inguinal approach (Mader *et al.*, 1999). The authors felt the less invasive inguinal fossa approach was the best option for this patient given his historic anemia and the fact that recent DECT imaging did not indicate any other bladder lesions were present.

Beyond surgery, lithotripsy with holmium:yttrium-aluminum-garnet (YAG) lasers has been investigated in tortoises with uroliths. This technique is likewise not without risks, and acute death was seen after lithotripsy in a tortoise, with evidence of acute cystitis and disseminated intravascular coagulation on necropsy (Keller *et al.*, 2015). Lithotripsy with a holmium:YAG laser is associated with additional concerns, including that large stones may

require repeated or long lithotripsy sessions (Nardini *et al.*, 2014). *In vitro* studies of holmium:YAG lithotripsy used on uric acid calculi also have shown that cyanide is produced as a by-product, which can present safety concerns (Teichman *et al.*, 1998; Corbin *et al.*, 2000). The amount of cyanide produced is dependent on total laser energy delivered; as such, this technique can be safe for the smaller urate stones (Zagone *et al.*, 2002). Because large stones can occupy an entire bladder lobe in chelonians, the amount of cyanide produced by lithotripsy may not be safe.

Given that other interventions are invasive and can pose a significant risk to chelonian patients, it is worth investigating medical management of uroliths in these animals. A review article of human uric acid urolithiasis showed that medical management of uroliths with oral alkalization therapy was highly effective as treatment of uric acid stones, resulting in resolution of existing uroliths through dissolution and prevention of recurrence by maintaining an alkaline environment not amenable to new calculus formation (Shekarriz and Stoller, 2002). Oral treatment in humans usually consists of oral sodium bicarbonate or more recently, potassium citrate, and treatment can range from 4 wk to 6 months (Cicerello, 2018). Sodium bicarbonate is currently less favored as a

dissolution agent as it increases excretion of calcium and sodium which may predispose patients to development of calcium oxalate stones (Sakhaee *et al.*, 1983). In feline and canine patients with urate uroliths, current consensus recommendations from the American College of Veterinary Internal Medicine suggest medical dissolution should be considered in a stable patient without concurrent disease, reserving invasive surgical removal to patients that fail or cannot tolerate medical management (Lulich *et al.*, 2016). Current recommendations for canine and feline urate uroliths recommend that dissolution should be achieved through dietary modification via feeding of a purine-restricted, alkalizing, diuretic diet (Lulich *et al.*, 2016). Purine-restricted commercial tortoise diets are not readily available; however, working with a veterinary nutritionist may allow for this diet. This approach was not done in this case. Potassium citrate supplementation is recommended in dogs and cats with persistently acidic urine (Lulich *et al.*, 2016). The dose of potassium citrate that was used in this case was derived from human and domestic animal doses (Pak *et al.*, 1986; Bartges *et al.*, 1999). Conversely, high levels of dietary potassium may be hazardous to a tortoise's health. Unlike some other desert reptiles, desert tortoises lack salt glands, meaning they must excrete excess potassium through their urinary system, losing water or proteins in the process of metabolizing potassium-rich plants (Ofstedal *et al.*, 2002). The potassium excretion potential (PEP) is a measure of the water, nitrogen, and potassium levels in a plant and how these affect the ability of a tortoise to efficiently excrete potassium. Wild desert tortoises are documented to preferentially consume plant species with a positive PEP, meaning there is more water and nitrogen in the food than is needed to excrete the potassium in the food (Ofstedal *et al.*, 2002). This could mean that supplementing potassium may actually predispose a tortoise to making urinary calculi. In captive settings, water is not a limited resource; thus, potassium excretion may be less metabolically costly.

One study demonstrated urine pH for five species of tortoises (red-footed tortoise [*Chelonoidis carbonarius*], Indian star tortoise [*Geochelone elegans*], Bell's hinge-back tortoise [*Kinixys belliana*], marginated tortoise [*Testudo marginata*], and Mediterranean spur-thighed tortoise [*Testudo graeca*]) exhibiting normal activity, that is, not immediately postbrumation, ranged from 8.0 to 8.5 (Innis, 1997). In that same study and another of free-ranging desert tortoises, urine pH appears to be affected by seasonal variation in activity, with more acidic urine (~5.0–6.0 pH) being seen postemergence from brumation (Christopher *et al.*, 1994; Innis, 1997). In the fall, desert tortoises were seen again to have a reduced urine pH ( $5.7 \pm 0.03$ ), but this correlated with a rise in plasma and urine ketones. Urine pH has been used as an indicator of overall metabolic status, with anorexic animals demonstrating an acidic pH (Innis, 1997). In short, causes of acidic urine are hypothesized to be dehydration, protein catabolism, and ketogenesis (Divers and Innis, 2019). Serial monitoring of urine pH is one way of measuring improvement in

metabolic status following periods of anorexia in herbivorous tortoises (Divers and Innis, 2019). In the case presented here, a urine pH of 6.0 was deemed acidic based on reference values for the season of presentation (July reference range:  $6.9 \pm 0.05$ ; Christopher *et al.*, 1994). A pH of 9.0 was achieved and maintained during treatment duration, although the role of potassium citrate versus a general improvement in health is unknown. In addition to urinary alkalization, vibration therapy, or attachment of a personal massager to the plastron, was used to aid in stone dissolution. The use of vibration therapy has been described for management of a gastrointestinal tract impaction in a marginated tortoise (Nicholas and Warwick, 2011), but to the author's knowledge has not been described in the literature for urolith management in chelonian patients. In addition, this tortoise was soaked daily, which could have substantial impact if the tortoise was actively drinking throughout treatment, because diuresis alone could have aided in stone dissolution. Although long-term success was not achieved with medical management in this case, the initial reduction in urolith size at the recheck DECT 2 months later was promising. More research evaluating the ideal maintenance urine pH for dissolution of urate stones in chelonians is crucial. Research evaluating ideal patient selection for medical management of urate stones also should be performed as those with calcified stones or with concurrent renal failure may not be ideal candidates.

Cystoliths in chelonians can often be treated as incidental findings, especially when found in an otherwise nonclinical patient presenting for a routine exam. However, they should not be neglected because they will continue to enlarge and can contribute to significant mortality (Mader, 2005; Keller *et al.*, 2015). Surgical intervention can be a financial burden on owners of chelonians, and some owners and veterinarians may not feel comfortable with the risks of invasive surgery. This case study demonstrates a positive outcome initially following medical management of a large urate cystolith. Unfortunately, in this case, the long-term outcome was regrowth of the stone, necessitating surgery. The use of DECT was essential in not only confirming the presence of the cystolith in this case but also identifying the composition noninvasively. These diagnostic and therapeutic techniques are promising additions to the existing options for managing the common chelonian pathology of urolithiasis and are worthy of further research regarding their efficacy and safety in a wider variety of patients. Furthermore, the authors suggest that CT, or DECT if available, imaging should be considered for any debilitated desert tortoise to help assess for occult cystoliths.

## Literature Cited

- Amat AC, Gabriel B, Chee NW. 2012. Cystic calculi removal in African spurred tortoise (*Geochelone sulcata*) using transplastron coeliotomy. *Vet World*, 5(8):489–492.
- Andrabi Y, Patino M, Das CJ, Eisner B, Sahani DV, Kambadakone A. 2015. Advances in CT imaging for urolithiasis. *Indian J Urol*, 31(3):185–193.



- Bartges JW, Osborne CA, Lulich JP, Kruger JM, Sanderson SL, Koehler LA, Ulrich LK. 1999. Canine urate urolithiasis: etiopathogenesis, diagnosis, and management. *Vet Clin North Am Small Anim Pract*, 29(1):161–191.
- Basha MAA, AlAzzazy MZ, Enaba MM. 2018. Diagnostic validity of dual-energy CT in determination of urolithiasis chemical composition: in vivo analysis. *Egypt J Radiol Nucl Med*, 49(2):499–508.
- Chitty J, Raftery A. 2013. Uroliths. In Chitty J, Raftery A (eds): *Essentials of Tortoise Medicine and Surgery*. Wiley-Blackwell, Hoboken, NJ:299–301.
- Christopher MM, Brigmon R, Jacobson E. 1994. Seasonal alterations in plasma  $\beta$ -hydroxybutyrate and related biochemical parameters in the desert tortoise (*Gopherus agassizii*). *Comp Biochem Physiol A Mol Integr Physiol*, 108(2–3):303–310.
- Cicerello E. 2018. Uric acid nephrolithiasis: an update. *Urologia*, 85(3):93–98.
- Corbin NS, Teichman JM, Nguyen T, Glickman RD, Rihbany L, Pearle MS, Bishoff JT. 2000. Laser lithotripsy and cyanide. *J Urol*, 14(2):169–173.
- Divers SJ, Innis CJ. 2019. Urology. In Divers S, Stahl S (eds): *Mader's Reptile and Amphibian Medicine and Surgery*. 3rd ed. Elsevier, St. Louis, MO:624–648.
- Frye FL. 1972. Surgical removal of a cystic calculus from a desert tortoise. *J Am Vet Med Assoc*, 161(6):600–602.
- Hidas G, Eliahou R, Duvdevani M, Coulon P, Lemaitre L, Gofrit ON, Pode D, Sosna J. 2010. Determination of renal stone composition with dual-energy CT: in vivo analysis and comparison with x-ray diffraction. *Radiology*, 257(2):394–401.
- Holmes SP, Divers SJ. 2019. Radiography–Chelonians. In Divers S, Stahl S (eds): *Mader's Reptile and Amphibian Medicine and Surgery*. 3rd ed. Elsevier, St. Louis, MO:514–527.
- Innis CJ. 1997. Observations on urinalyses of clinically normal captive tortoises. *Proc ARAV*, 109–112.
- Kambadakone AR, Eisner BH, Catalano OA, Sahani DV. 2010. New and evolving concepts in the imaging and management of urolithiasis: urologists' perspective. *RadioGraphics*, 30(3):603–623.
- Keller, K. 2019. Urolithiasis (cystic calculi and cloacal uroliths). In Divers S, Stahl S (eds): *Mader's Reptile and Amphibian Medicine and Surgery*. 3rd ed. Elsevier, St. Louis, MO:1355–1356.
- Keller KA, Hawkins MG, Weber EP 3rd, Ruby AL, Guzman DS, Westropp JL. 2015. Diagnosis and treatment of urolithiasis in client-owned chelonians: 40 cases (1987–2012). *J Am Vet Med Assoc*, 247(6):650–658.
- Klaphake E, Gibbons PM, Sladky KK, Carpenter JW. 2018. Reptiles. In Carpenter J (ed): *Exotic Animal Formulary*. 5th ed. Elsevier, St. Louis, MO: 82–166.
- Leng S, Shiung M, Ai S, Qu M, Vrtiska TJ, Grant KL, Krauss B, Schmidt B, Lieske JC, McCollough CH. 2015. Feasibility of discriminating uric acid from non-uric acid renal stones using consecutive spatially registered low and high-energy scans obtained on a conventional CT scanner. *Am J Rad*, 204(1):92–97.
- Lulich JP, Berent AC, Adams LG, Westropp JL, Bartges JW, Osborne CA. 2016. ACVIM small animal consensus recommendations on the treatment and prevention of uroliths in dogs and cats. *J Vet Intern Med*, 30(5):1564–1574.
- Mader DR. 2005. Calculi: urinary. In Mader DR (ed): *Reptile Medicine and Surgery*. 2nd ed. WB Saunders Co., Philadelphia, PA:763–771.
- Mader DR, Bennett RA, Funk RS, Fitzgerald KT, Vera R, Hernandez-Divers SJ. 2005. Surgery. In Mader DR (ed): *Reptile Medicine and Surgery*. 2nd ed. WB Saunders Co., Philadelphia, PA:763–771.
- Mader DR, Ling GV, Ruby AL. 1999. Cystic calculi in the California desert tortoise (*Gopherus agassizii*): evaluation of 100 cases. *Proc ARAV*, 81–82.
- Mangone B, Johnson JD. 1998. Surgical removal of cystic calculi via the inguinal fossa and other techniques applicable to the approach in the desert tortoise, *Gopherus agassizii*. *Proc ARAV*, 87–88.
- Murray N, Darras KE, Walstra FE, Mohammed MF, McLaughlin PD, Nicolaou S. 2019. Dual-energy CT in evaluation of the acute abdomen. *RadioGraphics*, 39(1):264–286.
- Nardini G, Bielli M, Nicoli S, Corlazzoli D, Selleri P, Leopardi S, di Girolamo N. 2014. Endoscopic laser lithotripsy in chelonians: two cases. *Veterinaria*, 28(6):33–37.
- Ngo TC, Assimos DG. 2007. Uric acid nephrolithiasis: recent progress and future directions. *Rev Urol*, 9(1):17–27.
- Nicholas E, Warwick C. 2011. Alleviation of a gastrointestinal tract impaction in a tortoise using an improvised vibrating massager. *J Herpetol Med Surg*, 21(4):93–95.
- Nykamp SG. 2017. Dual-energy computed tomography of canine uroliths. *Am J Vet Res*, 78(10):1150–1155.
- Oftedal OT, Hillard L, Morafka DJ. 2002. Selective spring foraging by juvenile desert tortoises (*Gopherus agassizii*) in the Mojave Desert: evidence of an adaptive nutritional strategy. *Chelonian Conserv Biol*, 4:341–352.
- Pak CY, Sakhaee K, Fuller C. 1986. Successful management of uric acid nephrolithiasis with potassium citrate. *Kidney Int*, 30(3):422–428.
- Ravi KK, Ananthkrishnan L, Kambadakone A, Platt JF. 2017. Update of dual-energy CT applications in the genitourinary tract. *Am J Roentgenol*, 208(6):1185–1192.
- Sakhaee K, Nicar M, Hill K, Pak CY. 1983. Contrasting effects of potassium citrate and sodium citrate therapies on urinary chemistries and crystallization of stone-forming salts. *Kidney Int*, 24(3):348–352.
- Shekarriz B, Stoller ML. 2002. Uric acid nephrolithiasis: current concepts and controversies. *J Urol*, 168(4):1307–1314.
- Teichman JM, Vassar GJ, Glickman RD, Beserra CM, Cina SJ, Thompson IM. 1998. Holmium:YAG lithotripsy: photothermal mechanism converts uric acid calculi to cyanide. *J Urol*, 160(2):320–324.
- Wisnbaugh ES, Paden RG, Silva AC, Humphreys MR. 2014. Dual-energy vs conventional computed tomography in determining stone composition. *Urology*, 83(6):1243–1247.
- Zagone RL, Waldmann TM, Conlin MJ. 2002. Fragmentation of uric acid calculi with the holmium: YAG laser produces cyanide. *Lasers Surg Med*, 31(4):230–232.